



Multicolor photoluminescent carbon nanodots regulated by degree of oxidation for multicolor patterning, invisible inks, and detection of metal ions

Bing Chen · Houpeng Xie · Sui Wang · Zhiyong Guo · Yufang Hu · Hongzhen Xie

Received: 6 December 2018 / Accepted: 19 March 2019 / Published online: 9 April 2019
© Springer Nature B.V. 2019

Abstract A strategy for preparing multicolor photoluminescent carbon nanodots (CNs) has been proposed. Using three types of phenylenediamine and methacrylic acid as raw materials and ethanol as a solvent, a series of novel CNs were synthesized by solvothermal one-pot method. Prepared CNs showed bright green, yellow, and indigo blue fluorescence under ultraviolet (UV) light, respectively. Three types of CNs were spherical-like nano-sized particles, and their particle sizes were approximately 5 nm, 10 nm, and 10 nm, respectively. The optical properties of CNs were characterized using ultraviolet visible spectra and fluorescence spectra. The microscopic morphology was characterized by transmission electron microscopy (TEM) and dynamic light scattering (DLS). The elemental composition was characterized by Fourier transform infrared spectroscopy (FT-IR) and X-ray photoelectron spectra (XPS). We proposed that the different fluorescence emissions of CNs might be attributed to the surface oxygen content of the CNs. The CNs could also be applied for multicolor patterning and polymer films, invisible inks, and detection of metal ions.

Keywords Carbon nanodots · Photoluminescence · One-pot synthesis · Fluorescent inks · Detection of metal ions

Introduction

Carbon-based nanoparticles, a new type of fluorescent nanoparticles, have emerged in recent years. The nanomaterials not only have excellent optical properties and nanometer size but also have good biocompatibility, environmental protection, and low toxicity (Kumar et al. 2017; L et al. 2015; Sahu et al. 2012; Wang et al. 2011a). These fluorescent carbon-based nanomaterials are mainly classified into carbon quantum dots (CQDs) (Dong et al. 2012; Lim et al. 2015), carbon nanodots (CNs) (Li et al. 2013), graphene quantum dots (GQDs) (Pan et al. 2010; Peng et al. 2012), and polymer quantum dots (PCDs) (Tao et al. 2017; Zhu et al. 2013b). The carbon dot materials have been applied in various fields based on their fascinating photoluminescent characteristics, such as bioimaging (Gong et al. 2016; Mewada et al. 2014), fluorescent inks (Qu et al. 2012; Liu et al. 2016), electrochemical sensing (Carrara et al. 2017; Liang et al. 2014), light-emitting devices (Sathyajith Ravindran et al. 2003), and heavy metal ions detection (Choudhary et al. 2016; Li et al. 2015; Yan et al. 2014; Zhang et al. 2015).

Many strategies of preparing carbon dots have been developed, including hydrothermal synthesis (Yuan et al. 2015; Zhu et al. 2015), chemical oxidation (Qiao et al. 2010), microwave synthesis (Wang et al. 2011b),

Electronic supplementary material The online version of this article (<https://doi.org/10.1007/s11051-019-4515-4>) contains supplementary material, which is available to authorized users.

B. Chen · H. Xie · S. Wang (✉) · Z. Guo · Y. Hu · H. Xie
Faculty of Materials Science and Chemical Engineering, State Key Laboratory Base of Novel Functional Materials and Preparation Science, Ningbo University, Ningbo 315211, People's Republic of China
e-mail: wangsui311@163.com

ultrasonic synthesis (Ma et al. 2012), and laser synthesis (Hu et al. 2011). Among them, the hydrothermal synthesis approach has been widely used due to its facility and rapidity. At present, there were two main sources of synthesis of carbon dots. One of them was bioprotein, in which mainly contains proteins and amino acids, such as milk (Wang and Zhou 2014), leaves, and flowers of plants (Feng et al. 2015b; Zhu et al. 2013a).

For example, Gao et al. (2014) hydrothermally treated the willow leaf to synthesize nitrogen-doped carbon dots (n-CDs). The n-CDs showed strong blue fluorescence that could be directly used as a fluorescent ink and possessed excellent electro-catalytic activity. The other carbon sources were organic alcohol, organic acid, organic amine, and so forth (Kozák et al. 2013; Shi et al. 2016; Li et al. 2010). Liu et al. (2012) reported a general strategy for the preparation of nitrated carbon dots (CNDs) by microwave heating organic amines in the presence of acid. The obtained CNDs can be used as a mimetic peroxidase for colorimetric detection of H_2O_2 and glucose.

Although many carbon dot materials with various photoluminescence properties have been reported, the mechanism of different fluorescence emission of various carbon dots remains unclear. At present, two more mature mechanisms are quantum size effect (Sarkar et al. 2016; Yu et al. 2013) and surface state that leads to different PL emission states (Bao et al. 2015). Jiang et al. (2015) prepared three types of CDs possessing different fluorescence emissions. The research result suggested that the difference in fluorescence emission of CDs might be caused by the difference in particle size and nitrogen content. Ding et al. (2016) strongly explored the PL mechanism of CDs. Their study demonstrated that several CDs have different surface states due to their different degrees of oxidation, resulting in different PL states.

Herein, we synthesized six types of CNs using m-phenylenediamine (or o-phenylenediamine or p-phenylenediamine) and methacrylic acid as the carbon source by a facile and rapid one-pot solvothermal method. These fluorescent CNs with different colors were prepared by adjusting the reaction precursor and reaction temperature. By characterizing the particle size and surface state of the three CNs, we proposed a possible PL mechanism that three CNs had the difference in fluorescence emission. Moreover, prepared CNs were applied as fluorescent inks and used to detect metal ions.

Experimental section

Chemicals and instruments

Methacrylic acid (MAA), m-Phenylenediamine (mPD), o-Phenylenediamine (oPD), p-Phenylenediamine (pPD), polyvinyl alcohol (PVA), quinine sulfate, and rhodamine 6G were obtained from Aladdin (Shanghai, China). $CuSO_4$, $FeCl_2 \cdot 4H_2O$, $FeCl_3 \cdot 6H_2O$, $CoCl_2 \cdot 6H_2O$, $Pb(NO_3)_2$, $CdCl_2$, $Cr(CH_3COO)_3 \cdot 6H_2O$, $NiSO_4 \cdot 6H_2O$, $MnSO_4$, $AgNO_3$, $Zn(CH_3COO)_2$, $Al_2(SO_4)_3$, $HgSO_4$, and alcohol were purchased from Sinopharm Chemical Reagent Co., Ltd. (Shanghai, China). All other chemicals were of analytical grade and used without further purification.

Photo images were recorded with a digital camera (Canon EOS 600D, Tokyo, Japan). The UV-visible absorption spectra were recorded by using UV-visible spectrophotometer (Shimadzu 3100, Tokyo, Japan). The fluorescence spectra were obtained using molecular fluorescence spectrometer (Hitachi F-4600, Tokyo, Japan). SEM morphology photographs were obtained by using field-emission scanning electron microscope (Hitachi S4800, Tokyo, Japan). TEM photographs were obtained by using transmission electron microscopy (Hitachi H7650, Tokyo, Japan). Dynamic light scattering (DLS) was measured by using laser nanoparticle size analyzer (Malvern Zetasizer Nano ZS90, Shanghai, China). FT-IR analysis was carried out with Fourier transform infrared (FT-IR) spectrometer (Nicolet 6700, Wisconsin, USA). X-ray photoelectron spectra (XPS) were tested using photoelectron spectrograph (ThermoFisher ESCALAB 250, Shanghai, China). Solutions were centrifuged using a high-speed centrifuge (H1650, Hunan xiangyi Laboratory Instrument Development Co., Ltd., Changsha, China). UV light source was provided by the ultraviolet analyzer (Hangzhou Qiwei Instrument Co., Ltd., Hangzhou, China).

Synthesis of a series of CNs

Three types of CNs (M/m1-CN, M/o1-CN, and M/p1-CN) were prepared by one-pot solvothermal synthesis method. In brief, 0.32 mL MAA and 0.2 g mPD (oPD or pPD) were dissolved in 20 mL alcohol and stirred for 10 min. Then, three types of solution were separately transferred into Teflon-lined stainless steel autoclave and heated at 200 °C for 3 h. After the autoclave cooled to room temperature, three viscous solids were obtained

and re-dispersed in ethanol. Yellow, red, and gray solutions (M/m1-CNs, M/o1-CNs, and M/p1-CNs, respectively) were obtained. And three types of solutions were centrifuged at 10000 rpm for 5 min (repeat three times) to remove agglomerated particles. Finally, three types of CNs were gained from the supernatant. In addition to the synthesis time became 8 h, other conditions were consistent with the above steps, and other three types of carbon nanodots (M/m2-CNs, M/o2-CNs, and M/p2-CNs) were obtained.

Measurement of fluorescence quantum yields

The fluorescence quantum yields (QYs) were calculated by using relative method (Jiang et al. 2015). Quinine sulfate (QYs = 54% in 0.1 M H₂SO₄) was chosen as the reference for M/o2-CNs. Rhodamine 6G (QYs = 95% in alcohol) was chosen as the reference for the M/m1-CNs and M/o1-CNs. The QYs of the three types of CNs were calculated using the following equation:

$$\varphi_x = \varphi_{\text{std}} I_x A_{\text{std}} \eta_x^2 / I_{\text{std}} A_x \eta_{\text{std}}^2 \quad (1)$$

Here, φ is the QYs of the testing sample, I is the measured integrated emission intensity, A is the optical density, and η is the refractive index of the solvent. The subscript “std” refers to the standard sample with known QYs, and “x” represents the unknown samples. Absorbance of samples was always kept below 0.1 at the excitation wavelength to minimize reabsorption effects.

Preparation and application of photoluminescent inks

Fluorescent photos of the three CN solutions were recorded using a digital camera under UV light. Meanwhile, some letters on filter paper were handwritten using an ink pen filled with solutions of CNs. Some figures of these patterns, letters, and paper artworks were obtained using a digital camera under daylight and UV light (365 nm), respectively.

Preparation of multicolor fluorescent CNs/PVA hybrid films

The multicolor fluorescent CNs/PVA hybrid films were prepared by hydrothermal treatment. Four gram PVA was dissolved in 30 mL deionized water and stirred for 5 min. Different mass ratios of CN solution with the same concentration were added in PVA solution, and

then the mixed solution was heated at 95 °C for 2 h under stirring. After the reaction was completed, viscous mixed solutions were covered on a glass plate and dried at room temperature. Finally, multicolor fluorescent CNs/PVA composite films were obtained.

Metal ions detection

Response property of metal ions to M/m1-CNs (M/o1-CNs and M/o2-CNs) for fluorescence was characterized by comparing the intensity of fluorescence emission. Two milliliter M/m1-CNs (0.01 mg/mL) solution was added to a centrifuge tube, and 0.1 mL of various metal ion solution (0.1 M) and deionized water (as blank contrast) were separately added into the above M/m1-CNs solution. These metal ions were Cu²⁺, Fe²⁺, Fe³⁺, Co²⁺, Pb²⁺, Cd²⁺, Cr³⁺, Ni²⁺, Mn²⁺, Ag⁺, Zn²⁺, Al³⁺, and Hg²⁺, respectively. The fluorescence emission spectra of mixed solutions with different metal ions were tested and recorded by molecular fluorescence spectrometer.

Results and discussions

Formation of CNs

The schematic diagram of the synthesis of fluorescent CNs is outlined in Fig. 1a. A possible mechanism may be that methacrylic acid and phenylenediamine undergo polymerization and dehydration at high temperature to form fluorescent carbon nanodots. Photographs of M/m1-CNs, M/o1-CNs, and M/o2-CNs are shown in Fig. 1b under daylight and UV light (365 nm), respectively. Solutions of the three types of CNs dispersed in ethanol showed yellow, red, and brown under daylight and emitted strong green, yellow, and indigo fluorescence under UV light (365 nm). Interestingly, the color of M/o2-CNs was observed for strong indigo under UV light (365 nm), which was different from M/o1-CNs. The situation provided a new idea to the synthesis of fluorescent carbon nanodots for other researchers in this field. That was, the fluorescence of carbon nanodots can be adjusted by changing the reaction time.

As shown in Fig. S1, the solutions of M/m2-CNs, M/p1-CNs, and M/p2-CNs were observed under daylight and UV light (365 nm), respectively. The solutions of M/m2-CNs showed yellow and transparent under daylight, but exhibited strong green under UV light

(365 nm), which was similar to the color of M/m1-CN. Fluorescence of the M/p1-CN and M/p2-CN was always weak. Therefore, three typical samples (M/m1-CN, M/o1-CN, and M/o2-CN) were researched as the main object.

Optical properties of CNs

Fluorescence properties, as the most important optical properties of CNs, which of three typical types of CNs (M/m1-CN, M/o1-CN, and M/o2-CN) were systematically studied (Fig. 2). Firstly, the emission spectra of the three types of CNs under different ranges of excitation wavelengths are displayed in Fig. 2 a and b. The maximum emission wavelengths of M/m1-CN, M/o1-CN, and M/o2-CN were located at 525 nm, 520 nm, and 350 nm with the excitation wavelengths in the range of 300–480 nm, 380–540 nm, and 260–400 nm, respectively. For the M/m1-CN (Fig. 2a), decreases in emission intensity were observed when different excitation wavelengths were excited, but a lesser extent of emission wavelength shifts. The result revealed that the M/m1-CN do not have an excitation-dependent property, which can be ascribed to surface uniformity of the CNs (Wang et al. 2017). The emission spectra of M/o1-CN and M/o2-CN showed typical excitation-dependent PL behavior. That was, the emission wavelength would redshift with the increasing of the excitation wavelength, which was usually the result of the combination of the surface emitter and central aromatic clusters (Xu et al. 2013; Zhang et al. 2015). Thus, the differences in fluorescence might be the result of different surface states of M/o1-CN and M/o2-CN, which can be actualized by changing their reaction time. Furthermore, the excitation spectra of the three types of CNs at the maximum emission wavelength were also investigated. The excitation spectra of M/m1-CN, M/o1-CN, and M/o2-CN are shown in Fig. 2d, which excitation wavelengths were located at 467 nm, 440 nm, and 310 nm, respectively. The UV-visible spectra of the three types of CNs, as shown in Fig. 2e, displayed similar characteristic peak in the range of 280–300 nm, which were attributed to the formation of an aromatic system of CNs (Kozák et al. 2013; Li et al. 2013). The fluorescence quantum yields of the M/m1-CN, M/o1-CN, and M/o2-CN were 9.6%, 36.0%, and 42.3%, respectively. Their different quantum yield of the three types of CNs might be attributed to the surface passivation (Al Awak et al. 2017; Feng et al. 2015a; Wang et al. 2010).

More effective surface passivation might cause higher fluorescence quantum yields, which corresponded with the degree of oxidation of these CNs.

Microscopic morphology of M/m1-CN, M/o1-CN, and M/o2-CN

Microscopic morphologies of the prepared M/m1-CN, M/o1-CN, and M/o2-CN were characterized by TEM as shown in Fig. 3a–c. The three types of CNs were spherical-like nano-sized particles, and their particle sizes were approximately 5 nm, 10 nm, and 10 nm, respectively. High-magnification TEM images in Fig. S2 A–C showed single particle of the three types of CNs. Obvious lattice fringes with a spacing about 0.21 nm were observed in Fig. S2 A–C, corresponding to the (100) in-plane lattice of graphene (Ding et al. 2016). Whereas, a spot of amorphous structures was also observed. These results indicated that these carbon nanodots had both crystalline and amorphous properties. The above results indicated the successful synthesis of carbon nanodots. To further verify the successful synthesis of carbon nanodots and their microscopic morphology, the particle size distribution of the three carbon dots was measured by DLS. The DLS of M/m1-CN, M/o1-CN, and M/o2-CN is shown in Fig. 3d–f, respectively. The particle size of the three types of CNs was in the range of 4–10 nm, 6–16 nm, and 6–12 nm, respectively. The average particle sizes of the three types of CNs were 5 nm, 10 nm, and 9 nm, respectively, corresponding to particle size of CNs observed from TEM images. To sum up, both TEM and DLS demonstrated successful synthesis of the three types of CNs with nanoscale characteristics. The luminescence of M/m1-CN and M/o1-CN with different colors might be due to their different quantum sizes (sizes of M/m1-CN and M/o1-CN were 5 nm and 10 nm, respectively). For M/o1-CN and M/o2-CN, the two CNs had the same particle size, but had difference in luminescence, which might be attributed to the different surface composition of the two CNs through different degrees of reaction.

FT-IR analysis

Figure 4a presented the FT-IR spectroscopy of the three types of CNs; it can be seen that the three types of CNs showed similar infrared characteristic absorption peak, indicating that the three types of CNs had similar chemical components. The characteristic peaks of M/m1-

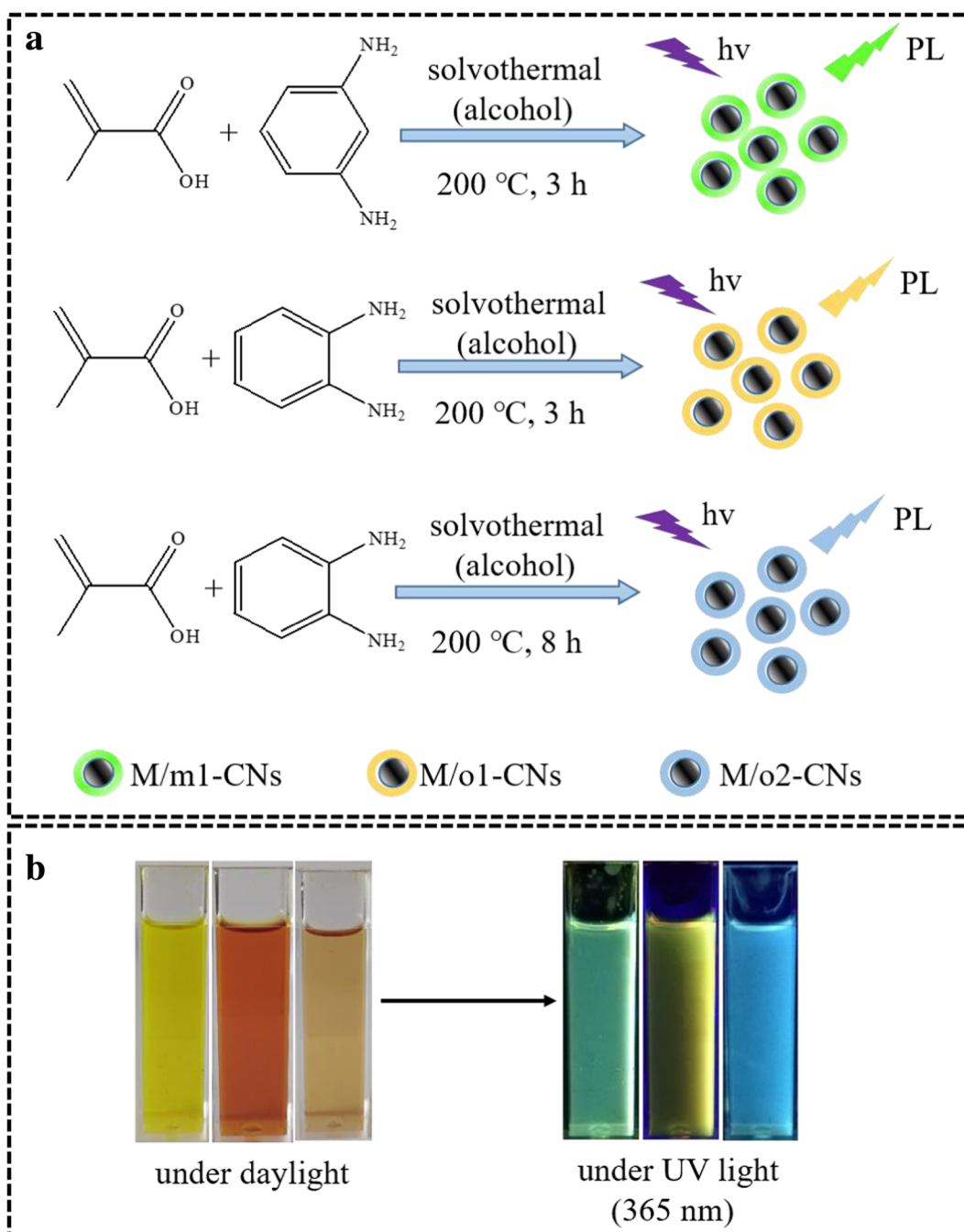


Fig. 1 Formation of M/m1-CNs, M/o1-CNs, and M/o2-CNs (a). M/m1-CNs, M/o1-CNs, and M/o2-CNs dispersed in ethanol solution under daylight and UV light (365 nm), respectively (b)

CNs, M/o1-CNs, and M/o2-CNs were at 3157 cm^{-1} , 3145 cm^{-1} , and 3129 cm^{-1} , respectively, which were attributed to the N–H vibration (Ding et al. 2016; Shi et al. 2016). For M/m1-CNs and M/o1-CNs, the characteristic peak at 3434 cm^{-1} was considered to be

caused by O–H vibration (Xue et al. 2016). However, for M/o2-CNs, characteristic absorption peak near 3400 cm^{-1} was not obvious, probably due to the low degree of oxidation of these CNs. Compared with the raw material (Fig. 4b), new characteristic peaks at

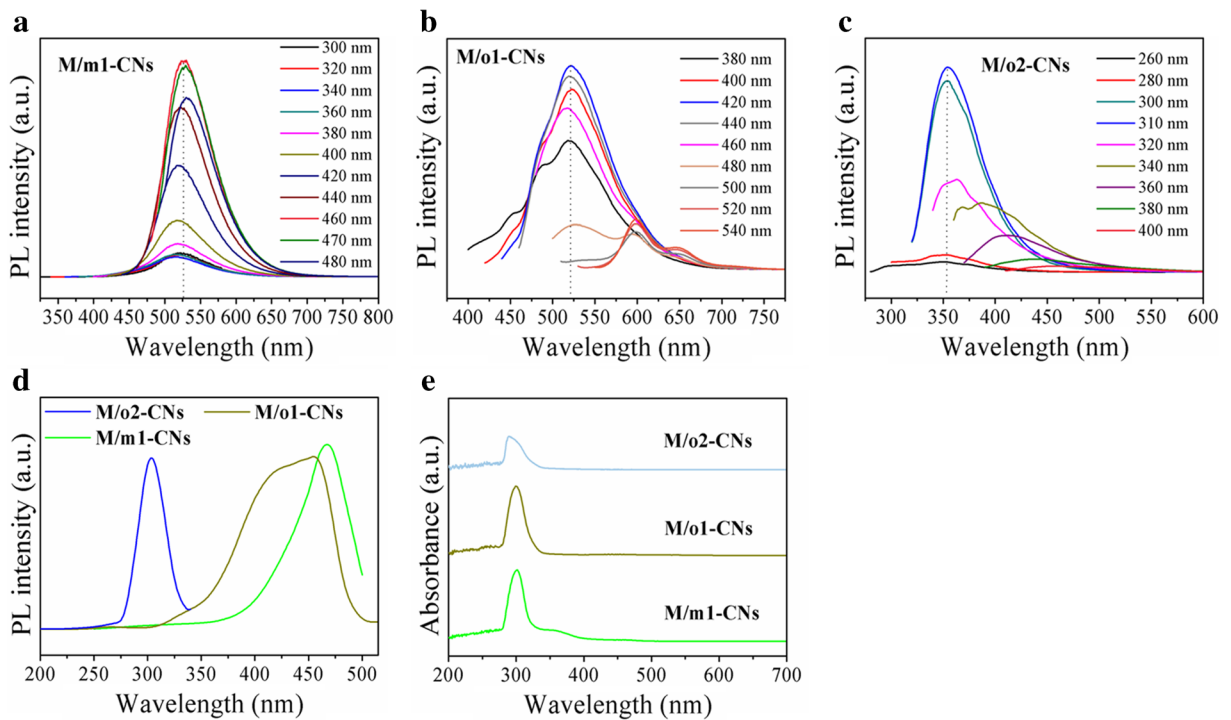


Fig. 2 Emission spectra (a–c) of M/m1-CNs, M/o1-CNs, and M/o2-CNs at different excitation wavelengths and excitation spectra (d) at the maximum emission wavelength. The UV-visible spectra of M/m1-CNs, M/o1-CNs, and M/o2-CNs (e)

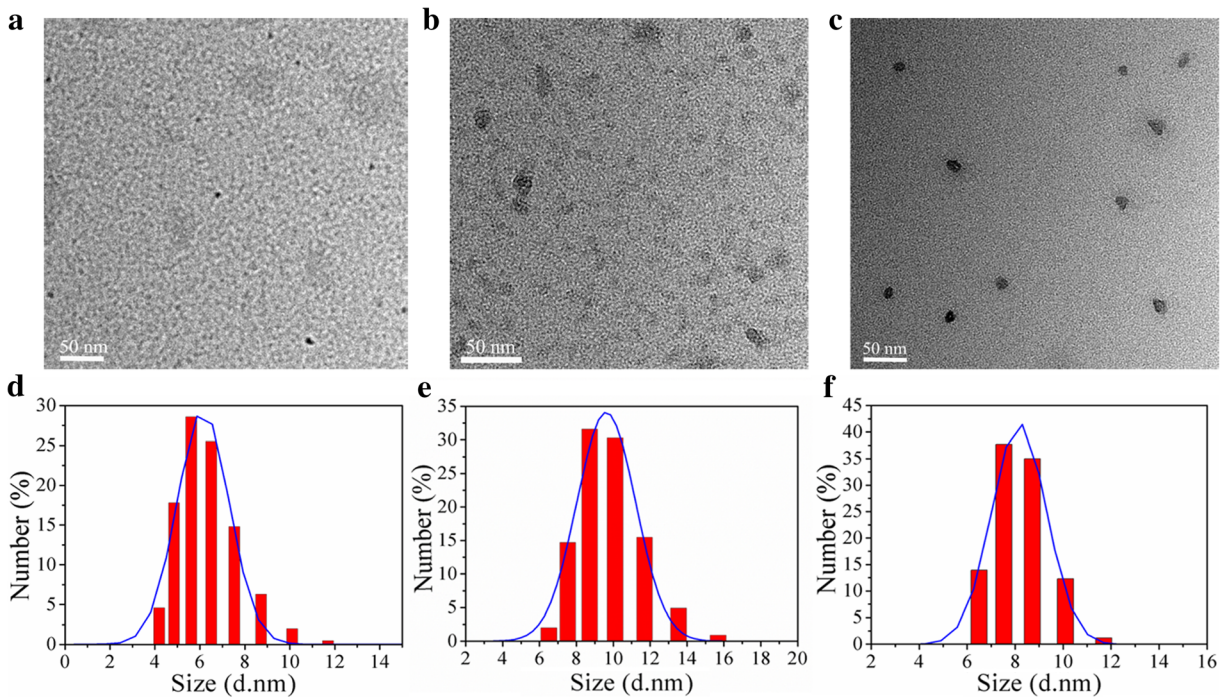


Fig. 3 TEM images of M/m1-CNs (a), M/o1-CNs (b), and M/o2-CNs (c). Particles size distribution of M/m1-CNs (d), M/o1-CNs (e), and M/o2-CNs (f) by DLS

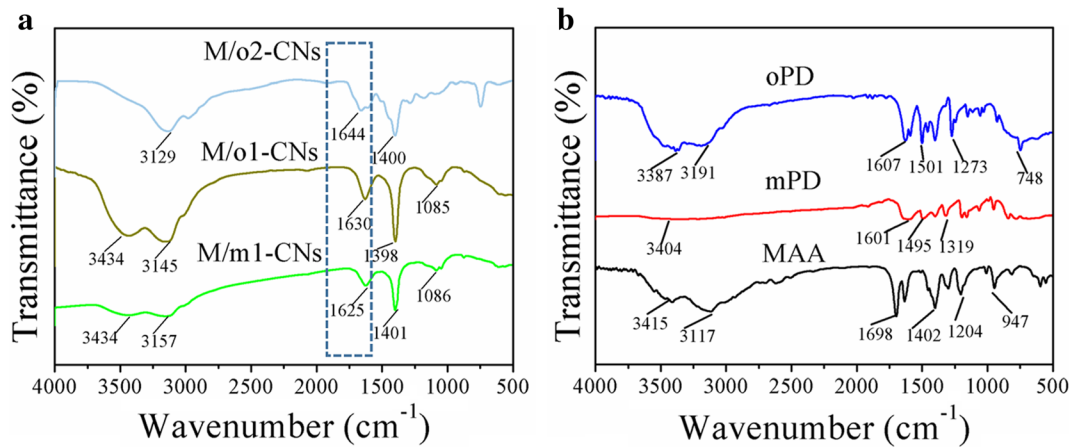


Fig. 4 FT-IR spectra of the three types of CNs (a) and raw materials (b)

1625 cm^{-1} , 1630 cm^{-1} , and 1644 cm^{-1} appeared for all three types of CNs, indicating formation of a new structure of CNs.

XPS analysis

The elemental composition of the three types of CNs was measured by XPS spectroscopy, as shown in Fig. 5. The result suggested that the three types of CNs have the same chemical element composition, namely C, N, and O. Three distinct peaks were at 285 eV, 398.4 eV, and 531.8 eV, which represented the C1s, O1s, and N1s of the three types of CNs, respectively. However, the

intensity of their C1s, O1s, and N1s peaks was different, indicating that the contents of C, N, and O elemental in the three types of CNs were different. High-resolution XPS C1s, N1s, and O1s spectra of M/m1-CNs, M/o1-CNs, and M/o2-CNs were obtained (Fig. S3). The C1s spectra of the three types of CNs can be decomposed into four peaks located at around 284.7, 286.0, 284.3, and 288.0 eV, corresponding to C–C, C–O, C=C, and C=N/C=O groups, respectively (Han et al. 2017). The C1s spectra revealed that three types of CNs were mainly composed of C–C and C–O groups, while C–N groups were few in the CNs. The N1s spectra of the three types of CNs indicated that the three CNs contain

Fig. 5 XPS survey spectra of the three types of CNs

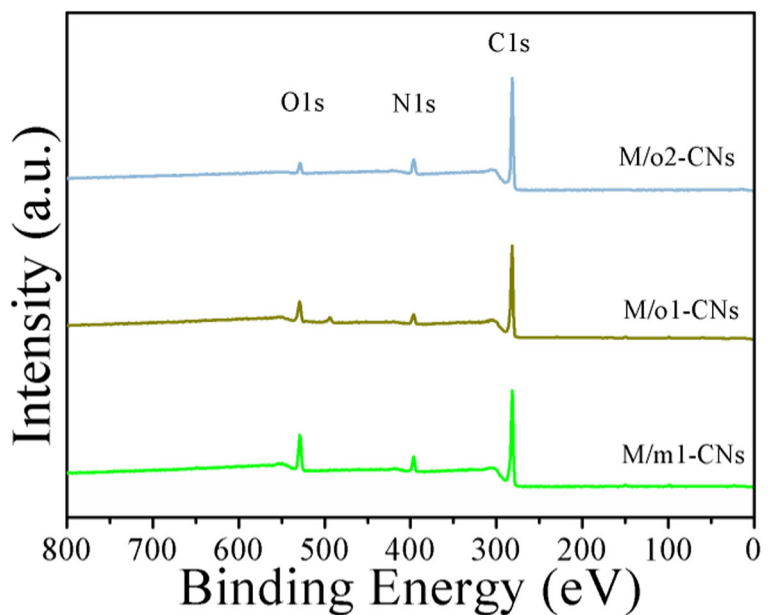


Table 1 The contents of C, N, and O atoms of the three types of CNs

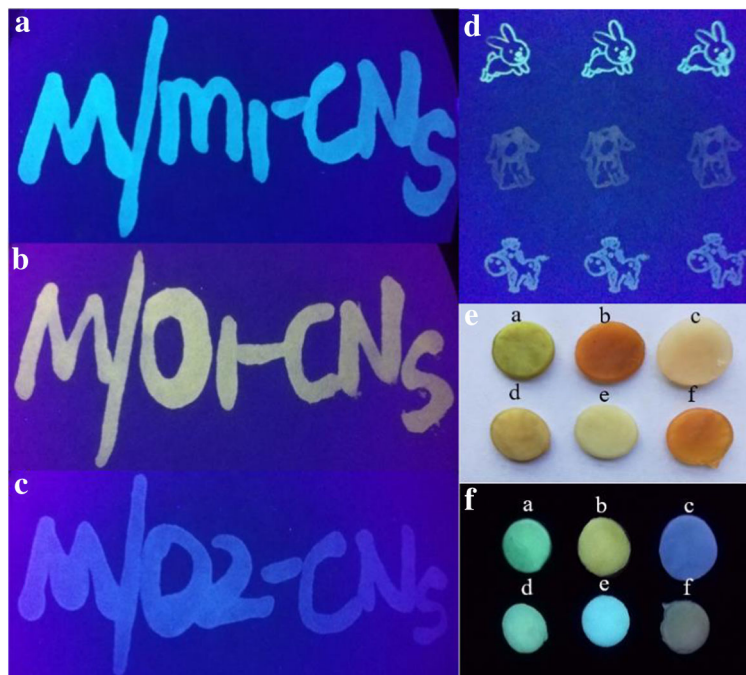
Sample	O (%)	N (%)	C (%)
M/m1-CN _s	12.15	7.03	80.81
M/o1-CN _s	8.74	6.22	85.04
M/o2-CN _s	3.69	8.88	87.43

different N groups on the CNs surface and different contents of similar functional groups. The O1s spectra of the three types of CNs can be decomposed into two peaks at 531.7 and 533.5 eV, representing C=O and C–O groups, respectively. The C=O group content in M/o2-CN_s was less than that in M/o1-CN_s. The above results clearly showed that the three types of CNs contain different functional groups and different contents of similar functional groups. The C, N, and O element content table is shown in Table 1. The content of the N elements of M/m1-CN_s, M/o1-CN_s, and M/o2-CN_s was 7.03%, 6.22%, and 8.88%, and corresponding O contents were 12.15%, 8.74%, and 3.69%, respectively. Interestingly, as emission of the CNs red shift, the O element content of CNs also increased. As a consequence, we believed that the difference of O element content might cause different fluorescence emissions of the CNs.

Study on colorful patterns of invisible fluorescent inks and multicolor CNs/PVA hybrid films

Based on excellent fluorescence properties of M/m1-CN_s, M/o1-CN_s, and M/o2-CN_s, the three types of CNs as fluorescent inks were applied to write letters in the filter paper. As shown in Fig. 6a–c, the corresponding letters were written with the M/m1-CN_s, M/o1-CN_s, and M/o2-CN_s fluorescent inks, respectively. The letters in Fig. 6 a, b, and c showed bright and clear green, yellow, and indigo fluorescence under UV light (365 nm), respectively. These fluorescent colors in filter paper correspond to fluorescent colors of corresponding CNs solution itself. Some signet dipped by CNs solution was used to print rabbit (green), puppy (yellow), and foal (indigo) patterns on the filter paper (Fig. 6d). The patterns on filter papers were barely visible under daylight, but showed bright and clear fluorescence under UV light (365 nm). These results indicated that the CNs as invisible inks were potentially applied for commerce such as anti-counterfeiting and enciphering-message. In addition, an interesting experiment was performed based on several different fluorescence colors of CNs. Different mass ratios CNs were added to the PVA gel to fabricate multicolor photoluminescent CNs/PVA hybrid gel films. The fluorescence of CNs/PVA hybrid film was regulated by the mass ratio of CNs. Photographs of the

Fig. 6 Letters were written with fluorescent inks made of CNs: M/m1-CN_s (a), M/o1-CN_s (b), and M/o2-CN_s (c). Patterns printed with inks made with three CNs (d). Multicolor CNs/PVA hybrid films under daylight (e) and UV light (f) (365 nm) (a) M/m1-CN_s; (b) M/o1-CN_s; (c) M/o2-CN_s; (d) M/m1-CN_s:M/o1-CN_s = 3:1 (w:w); (e) M/m1-CN_s:M/o2-CN_s = 2:1 (w:w); (f) M/o1-CN_s:M/o2-CN_s = 1:4 (w:w)



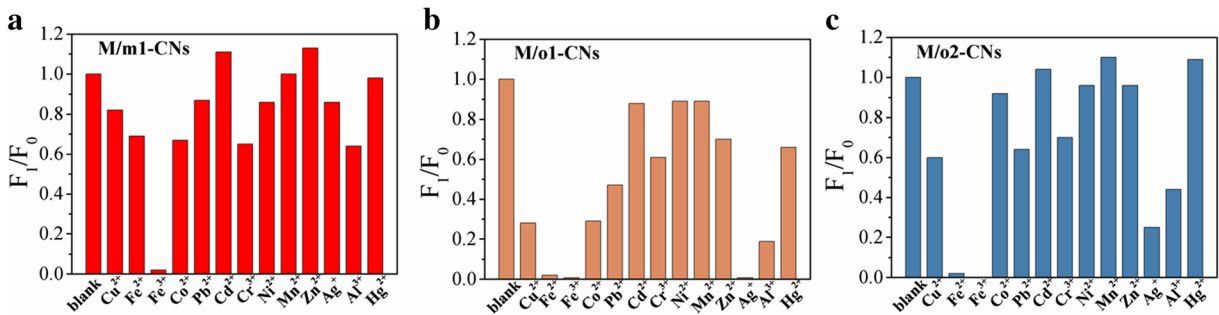


Fig. 7 Comparison of the fluorescence emission intensity of M/m1-CNs (**a**), M/o1-CNs (**b**), and M/o2-CNs (**c**) with metal ions (F_1 and F_0 were the fluorescence emission intensity of the CNs added with and without metal ions, respectively)

CNs/PVA gel film are shown in Fig. 6e, f under daylight and UV light (365 nm), respectively, in which a–f represented different mass ratios, respectively ((a) M/m1-CNs; (b) M/o1-CNs; (c) M/o2-CNs; (d) M/m1-CNs:M/o1-CNs = 3:1 (*w:w*); (e) M/m1-CNs:M/o2-CNs = 2:1 (*w:w*); (f) M/o1-CNs:M/o2-CNs = 1:4 (*w:w*)). Gels a, b, and c were green, yellow, and indigo fluorescence, respectively, corresponding the fluorescent colors of each CNs. Gels d, e, and f displayed light green, cyan, and brown fluorescence, respectively. The above results indicated that these CNs could be used for producing new multicolor gels.

Detection of metal ions

The fluorescence emission spectra and its standardizing of M/m1-CNs, M/o1-CNs, and M/o2-CNs solutions with different metal ions are shown in Fig. S4 (metal ions were Cu²⁺, Fe²⁺, Fe³⁺, Co²⁺, Pb²⁺, Cd²⁺, Cr³⁺, Ni²⁺, Mn²⁺, Ag⁺, Zn²⁺, Al³⁺, and Hg²⁺, respectively). As shown in Fig. 7a, Fe³⁺ had the strongest fluorescence quenching for M/m1-CNs compared with the rest of the metal ions, indicating that the M/m1-CNs had a specific recognition function for Fe³⁺. Therefore, the M/m1-CNs had potential application prospects in the field of detection of Fe³⁺. As shown in Fig. 7b, Fe²⁺, Fe³⁺, and Ag⁺ had stronger fluorescence quenching for M/o1-CNs, in addition to Cu²⁺, Co²⁺, and Al³⁺ which partly quenched fluorescence of M/o1-CNs. As shown in Fig. 7c, Fe²⁺ and Fe³⁺ had strong fluorescence quenching effect to M/o2-CNs, while Ag⁺ and Al³⁺ partly quenched fluorescence of M/o2-CNs. The quantitative detection of Fe³⁺ ions for M/m1-CNs was performed. The fluorescence intensity of the CNs decreased gradually with the increase of the concentration of Fe³⁺. There was a good semilogarithmic correlation between the quenching

efficiency (F_0/F_1) and the concentration of Fe³⁺ in the range from 10 to 300 μM (Fig. S5). Therefore, the concentration of Fe³⁺ could be calculated using the following calibration equation:

$$\text{Log}(F_0/F_1) = -0.00292 + 9.73493 \times 10^{-4}C \quad (R = 0.98734) \quad (2)$$

F_1 and F_0 were the fluorescence emission intensity of the M/m1-CNs added with and without metal ions, respectively, and C represented the concentration of Fe³⁺. The detection limit of Fe³⁺ was calculated to be 6 μM (at a S/N of 3).

Conclusions

In summary, we developed a facile, rapid, and green one-pot solvothermal synthesis method to manufacture multicolor fluorescence CNs. Different fluorescence emissions of CNs were regulated by changing the raw materials and reaction temperature. These CNs displayed bright and stable fluorescence under UV light (365 nm). Through the microscopic morphology and surface element analysis of CNs, we preliminarily think that the reason for the different fluorescence emission of CNs may be caused by the difference in particle size and the surface oxygen content. In addition, based on the excellent stable fluorescence characteristics of the carbon dots, we prepared invisible fluorescent inks and mixed fluorescence CNs/PVA hybrid films, which can potentially be used in commercial applications such as anti-counterfeiting, encrypted information, and luminescent devices. Moreover, we successfully applied CNs for the detection of metal ions, extending the application of CNs in the field of detection.

Funding information This research was supported by the National Natural Science Foundation of China (41576098, 81773483), the Science and Technology Department of Zhejiang Province of China (2016C33176, LGF18B070002), the Natural Science Foundation of Ningbo city (2017A610231, 2017A610228, 2017A610069), and the K.C. Wong Magna Fund in Ningbo University.

Compliance with ethical standards

Conflict of interest The authors declare that they have no conflict of interest.

References

- Al Awak MM, Wang P, Wang S, Tang Y, Sun Y-P, Yang L (2017) Correlation of carbon dots' light-activated antimicrobial activities and fluorescence quantum yield. *RSC Adv* 7:30177–30184. <https://doi.org/10.1039/c7ra05397e>
- Bao L, Liu C, Zhang ZL, Pang DW (2015) Photoluminescence-tunable carbon nanodots: surface-state energy-gap tuning. *Adv Mater* 27:1663–1667. <https://doi.org/10.1002/adma.201405070>
- Carrara S, Arcudi F, Prato M, De Cola L (2017) Amine-rich nitrogen-doped carbon nanodots as a platform for self-enhancing electrochemiluminescence. *Angew Chem* 56:4757–4761. <https://doi.org/10.1002/anie.201611879>
- Choudhary R, Patra S, Madhuri R, Sharma PK (2016) Equipment-free, single-step, rapid, “on-site” kit for visual detection of lead ions in soil, water, bacteria, live cells, and solid fruits using fluorescent cube-shaped nitrogen-doped carbon dots. *ACS Sustain Chem Eng* 4:5606–5617. <https://doi.org/10.1021/acssuschemeng.6b01463>
- Ding H, Yu SB, Wei JS, Xiong HM (2016) Full-color light-emitting carbon dots with a surface-state-controlled luminescence mechanism. *ACS Nano* 10:484–491. <https://doi.org/10.1021/acsnano.5b05406>
- Dong Y, Wang R, Li G, Chen C, Chi Y, Chen G (2012) Polyamine-functionalized carbon quantum dots as fluorescent probes for selective and sensitive detection of copper ions. *Anal Chem* 84:6220–6224. <https://doi.org/10.1021/ac3012126>
- Feng XT, Zhang F, Wang YL, Zhang Y, Yang YZ, Liu XG (2015a) Luminescent carbon quantum dots with high quantum yield as a single white converter for white light emitting diodes. *Appl Phys Lett* 107:213102–203106. <https://doi.org/10.1063/1.4936234>
- Feng Y, Zhong D, Miao H, Yang X (2015b) Carbon dots derived from rose flowers for tetracycline sensing. *Talanta* 140:128–133. <https://doi.org/10.1016/j.talanta.2015.03.038>
- Gao S, Chen Y, Fan H, Wei X, Hu C, Wang L, Qu L (2014) A green one-arrow-two-hawks strategy for nitrogen-doped carbon dots as fluorescent ink and oxygen reduction electrocatalysts. *J Mater Chem A* 2:6320–6326. <https://doi.org/10.1039/c3ta15443b>
- Gong X, Zhang Q, Gao Y, Shuang S, Choi MM, Dong C (2016) Phosphorus and nitrogen dual-doped hollow carbon dot as a nanocarrier for doxorubicin delivery and biological imaging. *ACS Appl Mater Interfaces* 8:11288–11297. <https://doi.org/10.1021/acsami.6b01577>
- Han L, Liu SG, Dong JX, Liang JY, Li LJ, Li NB, Luo HQ (2017) Facile synthesis of multicolor photoluminescent polymer carbon dots with surface-state energy gap-controlled emission. *J Mater Chem C* 5:10785–10793. <https://doi.org/10.1039/c7tc03314a>
- Hu S, Liu J, Yang J, Wang Y, Cao S (2011) Laser synthesis and size tailor of carbon quantum dots. *J Nanopart Res* 13:7247–7252. <https://doi.org/10.1007/s11051-011-0638-y>
- Jiang K, Sun S, Zhang L, Lu Y, Wu A, Cai C, Lin H (2015) Red, green, and blue luminescence by carbon dots: full-color emission tuning and multicolor cellular imaging. *Angew Chem* 54:5360–5363. <https://doi.org/10.1002/anie.201501193>
- Kozák O, Datta KKR, Greplová M, Ranc V, Kašlík J, Zbořil R (2013) Surfactant-derived amphiphilic carbon dots with tunable photoluminescence. *J Phys Chem C* 117:24991–24996. <https://doi.org/10.1021/jp4040166>
- Kumar A, Chowdhuri AR, Laha D, Mahto TK, Karmakar P, Sahu SK (2017) Green synthesis of carbon dots from *Ocimum sanctum* for effective fluorescent sensing of Pb²⁺ ions and live cell imaging. *Sensors Actuators B Chem* 242:679–686. <https://doi.org/10.1016/j.snb.2016.11.109>
- Li Q, Ohulchanskyy TY, Liu R, Koynov K, Wu D, Best A, Kumar R, Bonoiu A, Prasad PN (2010) Photoluminescent carbon dots as biocompatible nanoprobe for targeting cancer cells in vitro. *J Phys Chem C* 114:12062–12068. <https://doi.org/10.1021/jp911539r>
- Li W, Zhang Z, Kong B, Feng S, Wang J, Wang L, Yang J, Zhang F, Wu P, Zhao D (2013) Simple and green synthesis of nitrogen-doped photoluminescent carbonaceous nanospheres for bioimaging. *Angew Chem* 52:8151–8155. <https://doi.org/10.1002/anie.201303927>
- Li L, Yu B, You T (2015) Nitrogen and sulfur co-doped carbon dots for highly selective and sensitive detection of Hg (II) ions. *Biosens Bioelectron* 74:263–269. <https://doi.org/10.1016/j.bios.2015.06.050>
- Liang Z, Zeng L, Cao X, Wang Q, Wang X, Sun R (2014) Sustainable carbon quantum dots from forestry and agricultural biomass with amplified photoluminescence by simple NH₄OH passivation. *J Mater Chem C* 2:9760–9766. <https://doi.org/10.1039/c4tc01714e>
- Lim SY, Shen W, Gao Z (2015) Carbon quantum dots and their applications. *Chem Soc Rev* 44:362–381. <https://doi.org/10.1039/c4cs00269e>
- Liu S, Tian J, Wang L, Luo Y, Sun X (2012) A general strategy for the production of photoluminescent carbon nitride dots from organic amines and their application as novel peroxidase-like catalysts for colorimetric detection of H₂O₂ and glucose. *RSC Adv* 2:411–413. <https://doi.org/10.1039/c1ra00709b>
- Liu Y, Zhou L, Li Y, Deng R, Zhang H (2016) Highly fluorescent nitrogen-doped carbon dots with excellent thermal and photo stability applied as invisible ink for loading important information and anti-counterfeiting. *Nanoscale* 9:491–496. <https://doi.org/10.1039/C6NR07123F>
- Ma Z, Ming H, Huang H, Liu Y, Kang Z (2012) One-step ultrasonic synthesis of fluorescent N-doped carbon dots from glucose and their visible-light sensitive photocatalytic ability. *New J Chem* 36:861–864. <https://doi.org/10.1039/c2nj20942j>

- Mewada A, Pandey S, Thakur M, Jadhav D, Sharon M (2014) Swarming carbon dots for folic acid mediated delivery of doxorubicin and biological imaging. *J Mater Chem B* 2:698–705. <https://doi.org/10.1039/c3tb21436b>
- Pan D, Zhang J, Li Z, Wu M (2010) Hydrothermal route for cutting graphene sheets into blue-luminescent graphene quantum dots. *Adv Mater* 22:734–738. <https://doi.org/10.1002/adma.200902825>
- Peng J, Gao W, Gupta BK, Liu Z, Romero-Aburto R, Ge L, Song L, Alemany LB, Zhan X, Gao G, Vithayathil SA, Kaiparettu BA, Marti AA, Hayashi T, Zhu JJ, Ajayan PM (2012) Graphene quantum dots derived from carbon fibers. *Nano Lett* 12:844–849. <https://doi.org/10.1021/nl2038979>
- Qiao ZA, Wang Y, Gao Y, Li H, Dai T, Liu Y, Huo Q (2010) Commercially activated carbon as the source for producing multicolor photoluminescent carbon dots by chemical oxidation. *Chem Commun* 46:8812–8814. <https://doi.org/10.1039/c0cc02724c>
- Qu S, Wang X, Lu Q, Liu X, Wang L (2012) A biocompatible fluorescent ink based on water-soluble luminescent carbon nanodots. *Angew Chem* 51:12215–12218. <https://doi.org/10.1002/anie.201206791>
- Ravindran S, Chaudhary S, Colburn B, Ozkan M, CSO (2003) Covalent coupling of quantum dots to multiwalled carbon nanotubes for electronic device applications. *Nano Lett* 3: 447–453. <https://doi.org/10.1021/nl0259683>
- Sahu S, Behera B, Maiti TK, Mohapatra S (2012) Simple one-step synthesis of highly luminescent carbon dots from orange juice: application as excellent bio-imaging agents. *Chem Commun* 48:8835–8837. <https://doi.org/10.1039/c2cc33796g>
- Sarkar S, Banerjee D, Ghorai UK, Das NS, Chattopadhyay KK (2016) Size dependent photoluminescence property of hydrothermally synthesized crystalline carbon quantum dots. *J Lumin* 178:314–323. <https://doi.org/10.1016/j.jlumin.2016.05.033>
- Shi L et al (2015) Facile and eco-friendly synthesis of green fluorescent carbon nanodots for applications in bioimaging, patterning and staining. *Nanoscale* 7:7394–7401. <https://doi.org/10.1039/c5nr00783f>
- Shi L et al (2016) Carbon dots with high fluorescence quantum yield: the fluorescence originates from organic fluorophores. *Nanoscale* 8:14374–14378. <https://doi.org/10.1039/c6nr00451b>
- Tao S, Song Y, Zhu S, Shao J, Yang B (2017) A new type of polymer carbon dots with high quantum yield: from synthesis to investigation on fluorescence mechanism. *Polymer* 116: 472–478. <https://doi.org/10.1016/j.polymer.2017.02.039>
- Wang L, Zhou HS (2014) Green synthesis of luminescent nitrogen-doped carbon dots from milk and its imaging application. *Anal Chem* 86:8902–8905. <https://doi.org/10.1021/ac502646x>
- Wang X, Cao L, Yang ST, Lu F, Mezziani MJ, Tian L, Sun KW, Bloodgood MA, Sun YP (2010) Bandgap-like strong fluorescence in functionalized carbon nanoparticles. *Angew Chem* 49:5310–5314. <https://doi.org/10.1002/anie.201000982>
- Wang F, Xie Z, Zhang H, Liu C-Y, Zhang Y-G (2011a) Highly luminescent organosilane-functionalized carbon dots. *Adv Funct Mater* 21:1027–1031. <https://doi.org/10.1002/adfm.201002279>
- Wang X, Qu K, Xu B, Ren J, Qu X (2011b) Microwave assisted one-step green synthesis of cell-permeable multicolor photoluminescent carbon dots without surface passivation reagents. *J Mater Chem* 21:2445–2450. <https://doi.org/10.1039/c0jm02963g>
- Wang TY, Chen CY, Wang CM, Tan YZ, Liao WS (2017) Multicolor functional carbon dots via one-step refluxing synthesis. *ACS Sensors* 2:354–363. <https://doi.org/10.1021/acssensors.6b00607>
- Xu Y, Wu M, Liu Y, Feng XZ, Yin XB, He XW, Zhang YK (2013) Nitrogen-doped carbon dots: a facile and general preparation method, photoluminescence investigation, and imaging applications. *Chemistry* 19:2276–2283. <https://doi.org/10.1002/chem.201203641>
- Xue M, Zhan Z, Zou M, Zhang L, Zhao S (2016) Green synthesis of stable and biocompatible fluorescent carbon dots from peanut shell for multicolor living cell imaging. *New J Chem* 40:1698–1703. <https://doi.org/10.1039/C5NJ02181B>
- Yan F, Zou Y, Wang M, Mu X, Yang N, Chen L (2014) Highly photoluminescent carbon dots-based fluorescent chemosensors for sensitive and selective detection of mercury ions and application of imaging in living cells. *Sens Actuators B Chem* 192:488–495. <https://doi.org/10.1016/j.snb.2013.11.041>
- Yu X, Liu R, Zhang G, Cao H (2013) Carbon quantum dots as novel sensitizers for photoelectrochemical solar hydrogen generation and their size-dependent effect. *Nanotechnology* 24:335401. <https://doi.org/10.1088/0957-4484/24/33/335401>
- Yuan M, Zhong R, Gao H, Li W, Yun X, Liu J, Zhao X, Zhao G, Zhang F (2015) One-step, green, and economic synthesis of water-soluble photoluminescent carbon dots by hydrothermal treatment of wheat straw, and their bio-applications in labeling, imaging, and sensing. *Appl Surf Sci* 355:1136–1144. <https://doi.org/10.1016/j.apsusc.2015.07.095>
- Zhang Z, Sun W, Wu P (2015) Highly photoluminescent carbon dots derived from egg white: facile and green synthesis, photoluminescence properties, and multiple applications. *ACS Sustain Chem Eng* 3:1412–1418. <https://doi.org/10.1021/acssuschemeng.5b00156>
- Zhu L, Yin Y, Wang C-F, Chen S (2013a) Plant leaf-derived fluorescent carbon dots for sensing, patterning and coding. *J Mater Chem C* 1:4925–4932. <https://doi.org/10.1039/c3tc30701h>
- Zhu S et al (2013b) Highly photoluminescent carbon dots for multicolor patterning, sensors, and bioimaging. *Angew Chem Int Ed* 125:4045–4049. <https://doi.org/10.1039/C4RA16233A>
- Zhu J-H, Li M-M, Liu S-P, Liu Z-F, Li Y-F, Hu X-L (2015) Fluorescent carbon dots for auramine O determination and logic gate operation. *Sensors Actuators B Chem* 219:261–267. <https://doi.org/10.1016/j.snb.2015.05.032>

Publisher's note Springer Nature remains neutral with regard to jurisdictional claims in published maps and institutional affiliations.